Asymmetric rolling textures of aluminium studied with crystalline model implemented into FEM

M Wronski[1,2], K Wierzbanowski[1], B Bacroix[2] and P Lipinski[3]

[1] *AGH University of Science and Technology, Faculty of Physics and Applied Computer Science, al. Mickiewicza 30, 30-059 Kraków, Poland*

[2] *LSPM-CNRS.* Université Paris 13, 99, av. J.B. Clément, 93 430 Villetaneuse, France

[3] *LaBPS, ENIM, 1, Route d'Ars Laquenexy CS 65820, 57078 Metz Cedex 3, France*

E-mails: mwronskii@gmail.com, wierzbanowski@fis.agh.edu.pl, brigitte.bacroix@univ-paris13.fr, lipinski@enim.fr

Abstract. The goal of this work was to study the asymmetric rolling process using the Finite Element Method (FEM) coupled with the deformation model of polycrystalline material. The Leffers-Wierzbanowski (LW) model was selected to be implemented into FEM. This implementation enables a study of heterogeneous plastic deformation process, like asymmetric rolling, taking into account its crystallographic nature. Our aim was to examine the crystallographic texture and mechanical properties of asymmetrically rolled aluminium 6061. The simulation results are compared with experimental textures determined by X-ray diffraction. The advantages of asymmetrical rolling over symmetrical rolling are reduced rolling normal forces and rolling torques, improvement of microstructure and producing the homogeneous crystallographic texture.

1. Introduction

Asymmetric rolling (AR) is a promising forming technique offering numerous possibilities of material properties modification and the improvement of technological process parameters. The geometry of this process can be realized using existing rolling mills, commonly used in symmetric rolling (SR). AR can provide a large volume of a deformed material which is its advantage. Moreover, AR can be useful for industrial applications because it reduces the applied rolling forces and torques, changes the rolled plate shape and modifies the microstructure [1-4]. AR is a rolling process in which outer velocities of the upper and lower rolls are different. It can be achieved in different ways. AR studied in this work was realized using two identical rolls, of 180 mm diameter, driven by independent motors and rotating with different angular velocities ω_1 and ω_2. This ensured a wide range of rolling asymmetry. Asymmetry of the process is described by the parameter $A=\omega_1/\omega_2$. In the present work the modifications of crystallographic texture and mechanical characteristics of aluminium samples, caused by AR, were studied using the Finite Element Method (FEM) coupled with a polycrystalline deformation model. Theoretical results were checked by comparison of predicted and experimental textures.

2. Implementation of Crystallographic Model into Finite Element Method

The implementation of a crystallographic model into FEM code is an important issue for the description of anisotropic behavior of metals, like during AR process. In this work the model of polycrystalline plastic deformation proposed by Leffers [5] and further developed by Wierzbanowski et al. [6-8] was used (LW model). This model was selected, because it is fast and relatively simple in its formulation. The elasto-plastic isotropic interaction between a grain and a surrounding material is expressed by the equation:

$$\dot{\sigma}_{ij} = \dot{\Sigma}_{ij} + L(\dot{E}^p_{ij} - \dot{\varepsilon}^p_{ij}) \qquad (1)$$

where σ_{ij} and ε^p_{ij} are the stress and plastic strain tensors of a grain, Σ_{ij} is the stress tensor applied to the sample, E^p_{ij} is the plastic strain tensor of the sample and L is a scalar interaction parameter. This equation is a simplified version of the equation derived by Hill [9]; the total strain was replaced by the plastic strain (correct for the ranges of deformation considered), and the four-rank interaction tensor was replaced by the scalar parameter L. A given slip system *[uvw](hkl)* can be activated if the resolved shear stress $\sigma_{[uvw](hkl)}$ reaches a

Content from this work may be used under the terms of the Creative Commons Attribution 3.0 licence. Any further distribution of this work must maintain attribution to the author(s) and the title of the work, journal citation and DOI.
Published under licence by IOP Publishing Ltd

critical value τ_c (the Schmid law): $\tau_c = \sigma_{[uvw](hkl)}$. During deformation τ_c increases due to the work hardening. The latter process was described by a hardening matrix with a magnitude obeying a nonlinear saturating law [10]. For each elementary act of slip system activation, with a small shear strain $\delta\gamma$, the increments of plastic strain: $\delta\varepsilon_{ij}^{p} = \frac{1}{2}(m_i n_j + m_j n_i)\delta\gamma$ and of lattice rotation: $\delta\omega_{ij}^{latt} = -\frac{1}{2}(m_i n_j - m_j n_i)\,\delta\gamma$ were calculated (**m** and **n** are unit vectors along the *[uvw]* slip direction and the *(hkl)* slip plane normal).

In the present work the FEM calculations were done using ABAQUS/Explicit software [11]. The crystallographic model (LW) was implemented into ABAQUS via the user subroutine VUMAT. A representative polycrystalline model sample was attached to each finite element. Calculation in ABAQUS software are carried out incrementally. The calculation sequence in VUMAT subroutine (where LW model is implemented), in each Gauss point is as follows:
- at the beginning of each calculation step the ABAQUS program transfers to the VUMAT procedure a total strain increment ΔE_{ij} to be attained in this step (it is calculated basing on a stress state from the end of the preceding step and is called Σ_{ij}^{old} in the present step),
- LW model performs the imposed deformation ΔE_{ij} and calculates a new resulting stress state, Σ_{ij}^{new}, which is transferred to ABAQUS (it will become Σ_{ij}^{old} at the beginning of the next step).
The logical scheme of these operations is shown in Fig. 1.

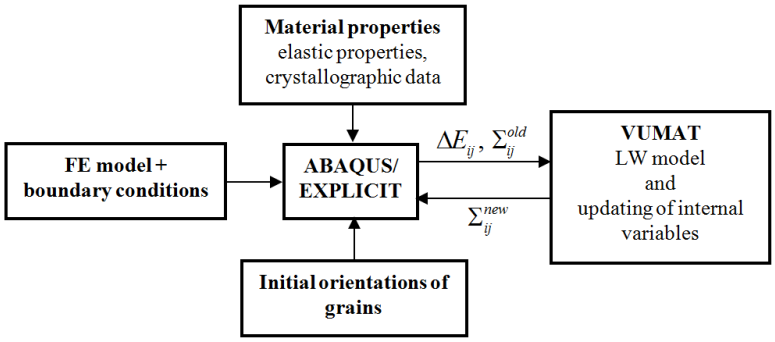

Fig. 1. *Interaction of LW model (included in VUMAT subroutine) with ABAQUS program.*

In order to decrease the number of finite elements the model of *plane strain* was used. The FEM sample contained 128 finite elements: 8 elements along ND, one element along TD and 16 elements along RD (8x1x16=128 elements). The initial textures of aluminium sample, determined by X-ray diffraction, was represented by 19200 grains - Fig. 4. A polycrystalline sample containing 150 grains was attached to each finite element of the C3D8R type (in each of 128 finite elements was 150 crystal grains - this gives the total number of 19200 grains representing a texture). When modelling AR, the Coulomb friction model was applied to describe the interaction of contacting surfaces (rolls and deformed material). The friction coefficient was estimated on the basis of the capture angle [12] and the value μ=*0.30* was used in the calculations. The rolls were modelled as rigid ones, using the *RIGID SURFACE option. In order to decrease the calculation time the process was artificially accelerated by increasing the rate of deformation. The total calculation time of the joint model was 0.275 s. The Mass Scaling factor equal to 5 was applied. The condition for quasi-static process in *Explicit mode* [11] was checked and fulfilled (the kinetic energy was negligible compared with the internal one).

3. Mechanical characteristics of asymmetrically rolled aluminium

The results presented in this section were obtained for the aluminium rolled to reduction of 36% with initial texture shown in Fig. 2. The calculated distributions of Σ_{13} and Σ_{33} components of the *internal stresses* in SR (A=1.0) and AR samples (A=1.05 and 1.3) are

shown in Fig. 3. One can note that during SR the shear stresses component, Σ_{13}, has the opposite sequence of signs on two surface layers (Fig. 3a-left). In contrast, when the degree of rolling process asymmetry increases, i.e., for A=1.3, there is no change of sign and the distribution of the Σ_{13} shear stress component becomes nearly homogeneous across the sample thickness (Fig. 3c-left). This results is in qualitative agreement with the calculations for isotropic material [13,14].

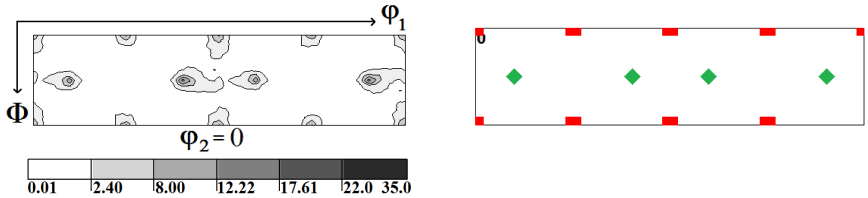

Fig. 2. *The crystallographic texture of the initial aluminium sample determined by X-ray diffraction. φ_2=0° sections are shown and orientations W (■) and B (◆) are marked.*

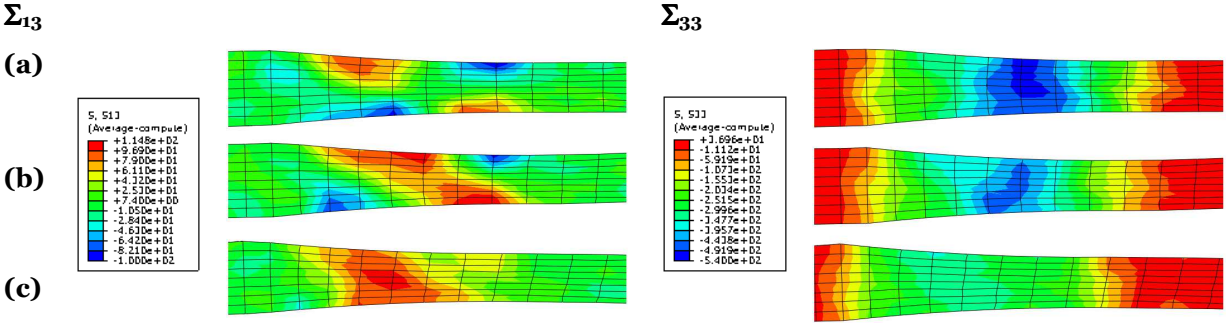

Fig.3. *Calculated distributions of Σ_{11}, Σ_{33} internal stress components during rolling with asymmetry ratios $A=\omega_1/\omega_2$ equal to: (a) 1, (b) 1.05 and (c) 1.3. Calculation was for polycrystalline aluminium rolled to 36% reduction in one pass (FEM+LW model).*

The distribution of the Σ_{33} normal component of *internal stress* for SR and AR is shown in Fig. 3-right. It is nearly homogeneous across the sample thickness and its magnitude decreases vs. rolling asymmetry, i.e., it is lower for AR (A=1.05 and A=1.3) than for SR (A=1.0). This effect explains the appearance of lower *residual stresses* in AR materials, as determined by diffraction measurements (cf. [15] and also [16-18])).
Also the external characteristics of the rolling process were examined. One of the advantages of AR, predicted by FEM calculations, is the reduction of the average normal force (F_{AR}) exerted on the sample surface. This is a consequence of reduction of the magnitude of the normal component of internal stress, Σ_{33}, exerted on the material by rolls (cf., Fig. 3-right). The predicted normal force (presented as the relative value F_{AR}/F_{SR}) vs. A, during rolling of polycrystalline aluminium, is shown in Fig. 4a. Also the *bend magnitude* versus A was calculated and it is shown in Fig. 3b. We note that sample bending can be reduced by an appropriate choice of rolling anisotropy (A). In our case its magnitude is strongly reduced starting from A=1.3. As expected, no bending was predicted for symmetric rolling, A=1.0. Another important variable is the total deformation work, W, supplied by the rolling mill to obtain a given deformation. It is presented as the ratio W_{AR}/W_{SR} , i.e., as the relative deformation work. This work increases with the degree of rolling asymmetry, A (Fig. 4c).

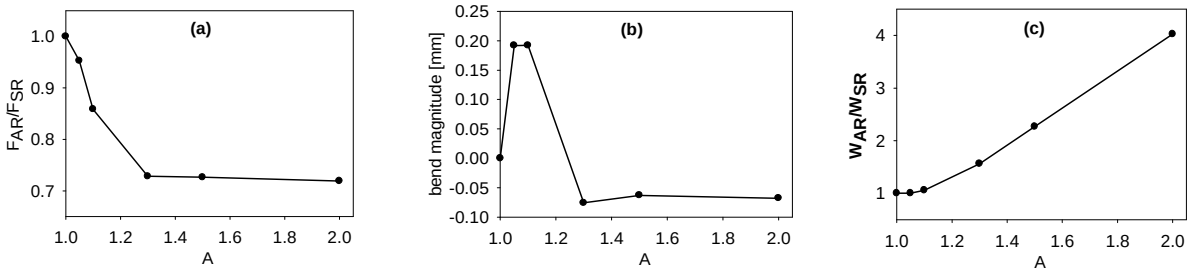

***Fig.4**. Mechanical characteristics versus $A=\omega_1/\omega_2$ predicted by FEM+LW model for polycrystalline aluminium (rolling reduction 36% in one pass): a) relative normal force (F_{AR}/F_{SR}), b) bend magnitude defined as deflection (in mm) at the end of 200 mm rolled plate, c) relative deformation work (W_{AR}/W_{SR}).*

3. Texture variation

Pole figures were determined in three layers of the rolled samples: in the top, bottom and central layers, using X-ray diffraction and corresponding ODFs were calculated [19]. Texture of the initial material is presented in $\varphi_2=0^o$ section of the Euler space (according to Bunge convention) and two main orientations are visible in this section: Brass (*B*) and Cubic (*W*) ones - Fig. 2. This material was next rolled symmetrically ($A=1$) and asymmetrically ($A=1.5$). The predicted rolling textures (by FEM+LW model) for three sample layers are compared with experimental textures of 6061 aluminium in Figs. 5, 6. Again only $\varphi_2=0^o$ sections, representative for texture modification, are shown in these figures. In the predicted SR texture (Fig.5a) we observe subtle shifts of texture maxima. Let us consider B orientation: in the top material layer the first two maxima of B component are shifted up and the two next ones - are shifted down (with respect to the red horizontal line drawn at $\Phi=45^o$), while the opposite sequence of shifts is observed in the bottom layer. These shifts do not occur in the centre layer of SR material: all equivalent B component maxima lie on the horizontal red line (Fig 5a-centre). The observed effect can be explained by the distribution of Σ_{13} shear stress component - Fig. 2a-left. In the top surface layer we observe the variation from positive to negative values of Σ_{13} and the opposite sequence appears in the bottom layer surface, while this stress component do not practically appear in the centre layer. Corresponding shifts of B component appear also in the experimental texture but with a lower magnitude - Fig. 5b. It can be shown that the discussed shifts of texture maxima are caused by texture rotations around transverse direction (TD) - cf. [20].

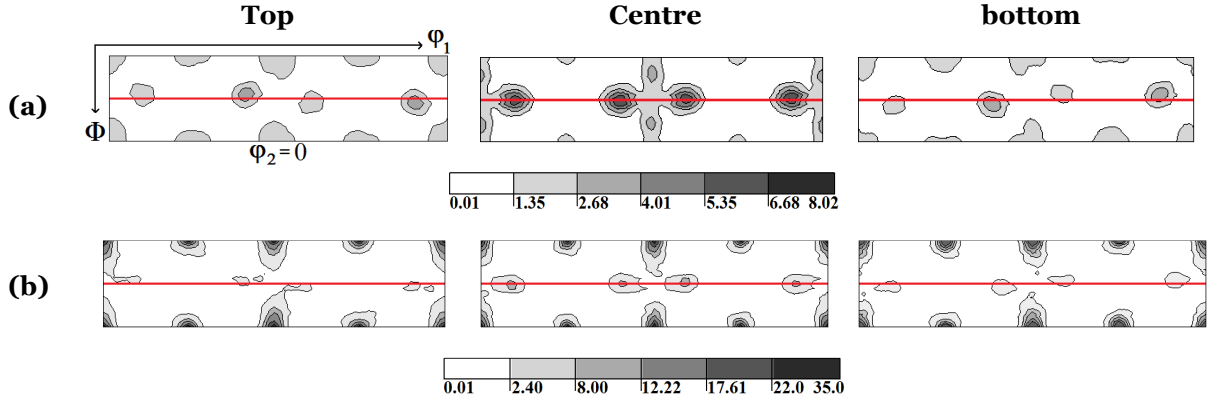

***Fig. 5**. Textures of symmetrically rolled aluminium ($A=\omega_1/\omega_2=1.0$) in top, centre and bottom material layers: a) predicted by FEM+LW model, b) determined by X-ray diffraction. $\varphi_2=0^o$ sections are shown and red line is located at $\Phi=45^o$.*

Another behaviour is observed in predicted textures of AR material (Fig.6) - the shifts of *B* maxima have the same character in all three examined material layers (the first two maxima are shifted up and two next ones - are shifted down) - Fig. 6a. The same effect appears is experimental textures, though with a smaller magnitude - Fig. 6b. Therefore, we conclude

that texture is much more homogeneous after AR process than after SR one. This behaviour can be explained by a nearly homogeneous distribution of the Σ_{13} shear stress component across the sample thickness- Fig. 2c-left.

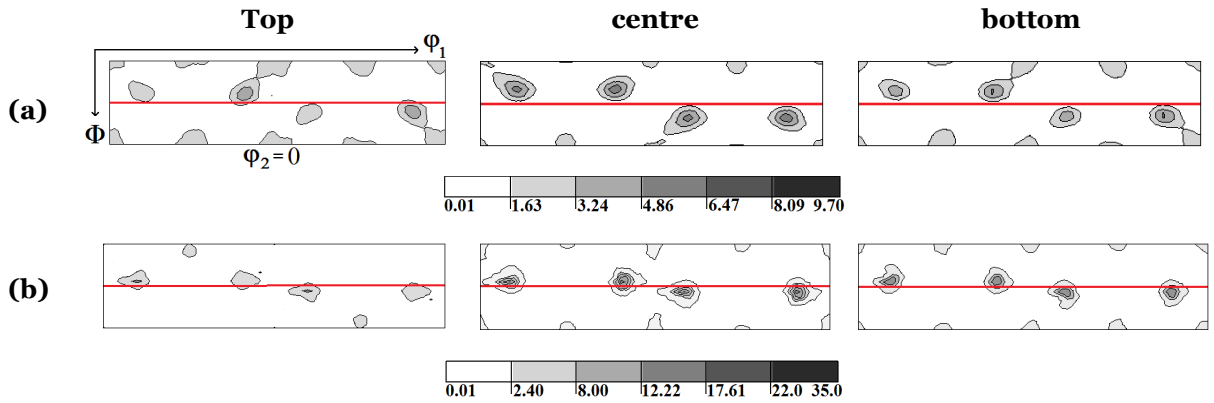

***Fig. 6**. Textures of asymmetrically rolled aluminium ($A=\omega_1/\omega_2=1.5$) in top, centre and bottom material layers: a) predicted by FEM+LW model, b) determined by X-ray diffraction. $\varphi_2=0^o$ sections are shown and red line is located at $\Phi=45^o$.*

The variation of texture across the material thickness was analyzed in function of distance from the top surface. The material studied by FEM+LW model was divided into eight layers, as shown in Fig. 7.

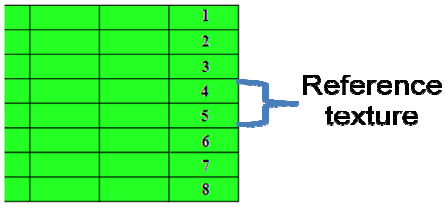

***Fig.7.** Division of the rolled material into eight layers used in FEM+LW calculations.*

The average texture of two central layers (No. 4 and 5) served as the reference one. Next, to compare a texture from a given layer with the reference one we used the correlation factor *R* (according to the procedure developed in [21]) which expresses the degree of similarity between two textures. *R* = 1 means that two textures being compared are identical, and *R=0* mean that textures are totally different. The calculated correlation factor *R* versus depth for different degrees of rolling asymmetry (*A*) is shown in Fig. 8. We note that the strongest variation of *R* appears in the case of SR, i.e., A=1.0. This is consistent with the character of shifts visible in Fig. 5. For higher degrees of asymmetry (*A*=1.5 and *A*=2.0) the variation of *R* becomes much more flat and *R* reaches the values around 0.9. This confirms the effect of texture homogenization across the sample thickness during AR.

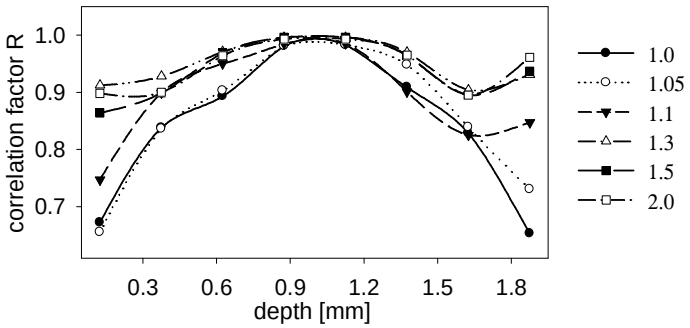

***Fig.8.** Correlation factor R expressing similarity of textures from different layers of aluminium sample with the reference SR texture of the centre layer, calculated by FEM+LW model. Results for $A=\omega_1/\omega_2$ equal to 1.0, 1.05, 1.1, 1.3, 1.5 and 2.0 are shown.*

Conclusions

The obtained theoretical and experimental results for rolled polycrystalline aluminium confirm that AR leads to:

- Texture modification- rolling texture are more homogeneous across the sample thickness after AR (they are homogeneously rotated around TD),
- Decrease of the applied rolling force due to a decrease of Σ_{33} internal stress component vs. rolling asymmetry (which is favorable for rolling mill durability),
- Modification of bend magnitude (bending can be reduced by appropriate choice of rolling asymmetry).

Acknowledgements

This study was financed by the Polish National Centre for Science (NCN) under decision numbers: DEC-2011/01/B/ST8/07394 and DEC-2011/01/D/ST8/07399.

References

[1] Gao H and Chen G 1998 Asymmetrical cold rolling realized on plain mill for steel sheet by laser-textured rolls, *Iron and Steel* **33** 63
[2] Lee S H and Lee G N 2001 Analysis of deformation textures of asymmetrically rolled steel sheets, *Int. J. Mech. Sci.* **43** 1997
[3] Wronski S et al. 2011 Analysis of textures heterogeneity in cold and warm asymmetrically rolled aluminium, *Mater. Character.* **62** 22
[4] Wronski S and Bacroix B 2014 Microstructure evolution and grain refinement in asymmetrically rolled aluminium, *Acta Mat.* **76** 404
[5] Leffers T 1968 Computer Simulation of the Plastic Deformation in Face-Centred Cubic polycrystals and the Rolling Texture Derived, *phys. stat. solidi* **25** 337
[6] Wierzbanowski K et al. 2007 Elasto-plastic models of polycrystalline material deformation and their applications, *Arch. Metall. Mater.* **52** 77
[7] Baczmanski A et al. 1995 Models of Plastic Deformation Used for Internal Stress Measurements, *Zeit. Metallkd.* **86** 507
[8] Wierzbanowski K et al., 2014 FCC rolling textures reviewed in the light of quantitative comparisons between simulated and experimental textures, *Crit. Rev. Solid State & Mater. Sci.* **39** 391
[9] Hill R 1965 A Self-Consistent Mechanics of Composite Materials, *J. Mech. Phys. Solids,* **13** 213
[10] Wierzbanowski K et al. 1999 Deformation Characteristics Important for Nucleation Process. Case of Low-Carbon Steels, *Archives of Metallurgy* **44** 183
[11] Hibbitt H.D, Karlson B.I, Sorensen D, 2004 *ABAQUS Example Problems Manual. Rolling of Thick Plates* (1.3.6) (*Dassault Systèmes)* pp 485-502
[12] Gudur P et al. 2008 A theoretical study on the application of asymmetric rolling for the estimation of friction, *Int. J. Mech. Sci.* **50** 315
[13] Wronski S et al. 2009 Texture heterogeneity of asymmetrically rolled low carbon steel, *Arch. Met. Mater* **54** 89
[14] Wronski S et al. 2010 Crystallographic Textures Variation in Asymmetrically Rolled Steel, *Mater. Sci. Forum* **638-642** 2811
[15] Wronski M et al. 2014 Modification of stress and texture distributions in asymmetrically rolled titanium, *Adv. Mater. Res.* **996** 688
[16] Baczmanski A et al. 1997 Anisotropy of Micro-Stresses Measured by Diffraction, *Revue de Metallurgie - Cahiers d'Informations Techniques* **94** 1467
[17] Baczmanski A et al. 1999 Internal Stresses in Two Phase Polycrystalline Materials, *Archives of Metallurgy* **44** 39
[18] Baczmanski A et al. 2006 New Type of Diffraction Elastic Constants for Stress Determination, *Mat. Sci. Forum* **524-525** 235
[19] Tarasiuk J et al. 1998 New Algorithm of Direct Method of Texture Analysis, *Cryst. Res. Technol.* **33** 101
[20] Wronski M et al. 2014 Texture variation in asymmetrically rolled titanium. Study by Finite Element Method with implemented crystalline model, *Int. J. Mech. Sci.* **87** 258
[21] Tarasiuk J and Wierzbanowski K 1996 Application of the Linear Regression Method for Comparison of Crystallographic Textures, *Phil. Mag. A* **73** 1083